EUROPEAN SOUTHERN OBSERVATORY
European Organisation for Astronomical Research in the Southern Hemisphere
Europäische Organisation für astronomische Forschung in der südlichen Hemisphäre
Organisation Européenne pour des Recherches Astronomiques dans l'Hémisphère Austral

Report:

Characterization of the OmegaCAM User-Provided Composite Filter NB_659

VST-MAN-OCM-?????-????

Issue: 1.2

Date: 30/08/2012

Prepared:	Mark Neeser	30/08/2012	
	Name	Date	Signature
Approved:			
	Name	Date	Signature
Released:			
	Name	Date	Signature

Change Record

Issue	Date	Sections Affected	Remarks
1.0	30/08/2012	All	Document creation
1.1	01/09/2012	All	Addition of long-term dome flat ratos
1.2	12/09/2012	All	Implementation of suggestions and corrections given by Dietrich Baade

Summary

- the NB_659 filter is described in documents provided by the `VPHAS+` consortium (Drew & Greimel (2009) and Martin (2011)).
- the NB_659 filter compares closely with the H_ALPHA filter in having similar throughputs and zeropoints. The raw dome flat flux levels differ by only 19.3 $\pm$ 12 ADU between the two filters, or 0.05% of the total flux. Furthermore, the difference remains constant over the entire 10 month time period between the beginning of operations and August 2012. The standard star zeropoints differ by only 0.22 $\pm$ 0.5 magnitudes between these two filters.
- the NB_659 filter has shown itself to be very stable during the time frame of 10 months between the beginning of OmegaCAM operations and the end of August, 2012. During this time, the NB_659 filter follows the H_ALPHA flux variations very closely and, when dome flat lamp and attenuation effects are removed, the raw dome flat flux levels of NB_659 fluctuate by less than 0.6%.

Contents

1 Introduction **5**

2 Description **6**

3 Comparison to the H_ALPHA Filter **7**

4 Long-Term Stability **9**

1 Introduction

This brief report intends to provide a short characterization of the narrow-band, composite filter provided by the VPHAS+ consortium. Full documentation, including laboratory testing, was provided by the VPHAS+ consortium Drew & Greimel (2009). This report will focus on two main aspects of NB_659: its comparison with the previously characterized Hα narrow-band filter (H_ALPHA) having similar properties, and its long-term stability.

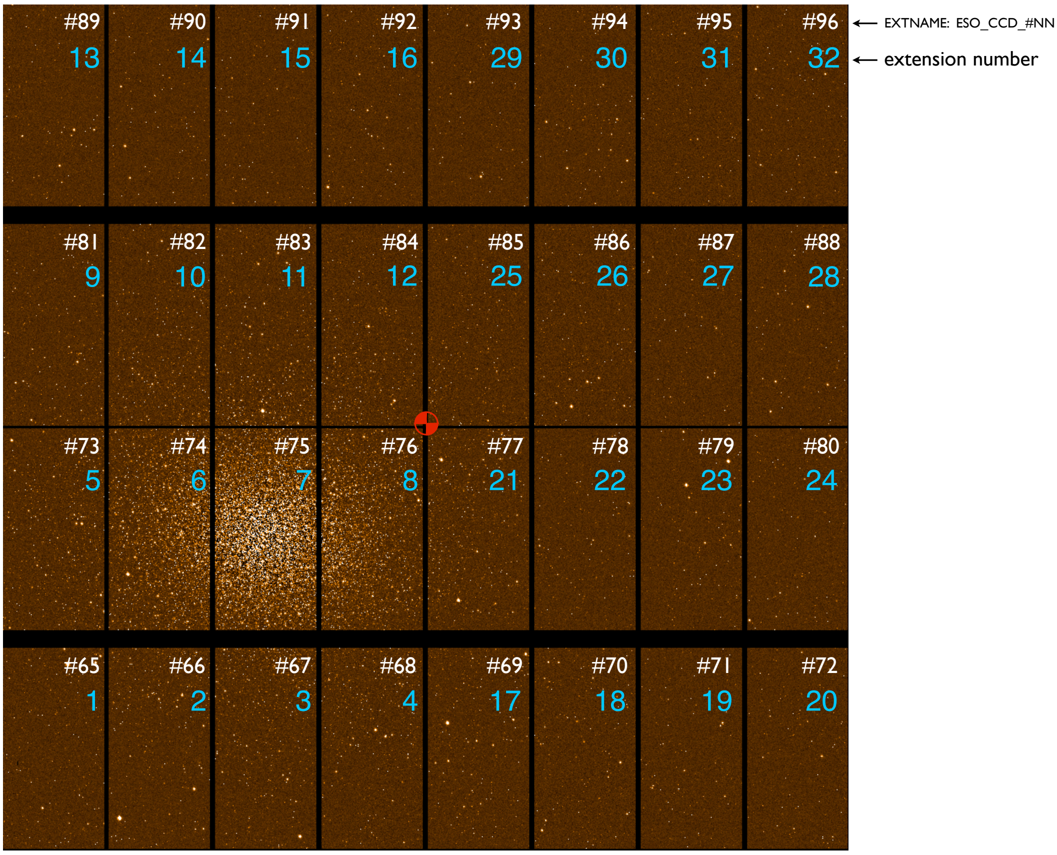

Figure 1: The detector layout mapping the positions of individual CCDs is given for reference.

2 Description

The four-segment Hα filter was procured by the `VPHAS+` consortium in June 2009 and is the distinctive narrow-band filter included in the VST public survey of the u, g, r, i and Hα photometric properties of the stellar populations of the southern Galactic Plane. The filter was manufactured to a specified central wavelength and FWHM of 658.8 nm and 10.7 nm, respectively (Drew & Greimel (2009)). Retesting of the filter was done in April 2011 and indicated that the filter transmission was unchanged (within $\pm 0.1\%$ in transmission and $\pm$ 0.2 nm in wavelength) after almost 2 years in storage (Martin (2011)). The nominal central wavelengths are 658.6 nm for three quadrants and 659.3 nm for one quadrant, with all quadrants having a FWHM of 10.5 nm (Mieske (2012)):

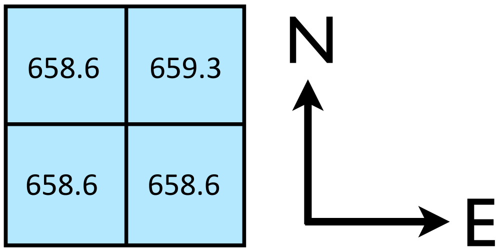

The Drew & Greimel (2009) and Martin (2011) reports argued that the transmission, optical quality, and wavelength properties of the NB_659 filter are adequate to fulfill all of the science goals proposed by the `VPHAS+` public survey.

As with all of the segmented filters of OmegaCAM, NB_659 is supported by a central + -shaped structure that is raised above the filter plane. As such, these filters exhibit a pronounced shadow due to this structure. This vignetting is sharply edged and can be seen in any full-field dome flat of NB_659 (see figure 2). The largest horizontal and vertical extent of this vignetting is 1384 and 1422 pixels, respectively, and can be effectively removed by dithering science exposures by 310 arcsec in both axes.

Finally, it is important to note that when the NB_659 filter arrived in Paranal it was quite dusty with some surface marking. Since the nature of the coating was not clear, it did not seem safe to attempt a cleaning of the filter. This report, by necessity, only takes into account the flat field and standard star properties of NB_659. Since filters in OmegaCAM are located far above the focal plane any effects of surface pollution will be sufficiently smeared out that their direct effects can escape detection.

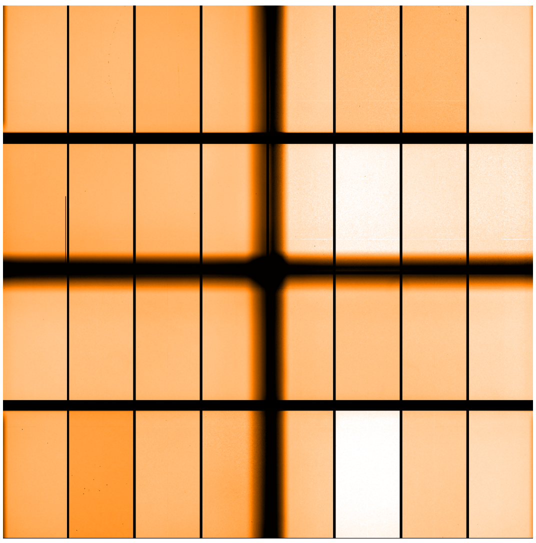

Figure 2: A full-field view of a raw NB_659 dome flat showing the large area vignetting that results from the central support of this segmented filter. The sizes of the horizontal/vertical vignetting is 1384 and 1422 pixels (296 and 304 arcsec), respectively. Thus, an X/Y dither of 310 arcsec is used to remove the vignetted area.

3 Comparison to the H_ALPHA Filter

An Hα filter already exists for OmegaCAM and was tested during instrument commissioning. This filter was delivered by the OmegaCAM consortium and samples the Hα line in four slightly overlapping redshift ranges: z = 0.00, 0.01, 0.02, and 0.03, with central wavelengths of 659.0 nm, 666.0 nm, 672.6 nm, and 679.1 nm, respectively, and a FWHM of 11.0 nm (Mieske (2012)).

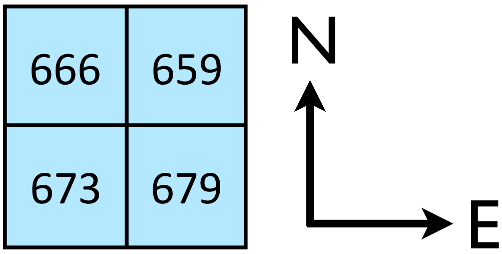

The H_ALPHA and NB_659 filters were both manufactured by Barr Associates, have very similar FWHM, and have central wavelengths that are, at most, separated by 20 nm. Thus, the NB_659 dome flat levels and zeropoints should be comparable to those of the H_ALPHA filter.

A ratio of two master dome flats, taken within two days of one another (NB_659 from 2012-08-22 and H_ALPHA from 2012-08-20), is shown in figure 3. The NB_659 dome flat (OC_MFLD_120822A_1_1_normal_normal_NB_659.fits) was divided by the H_ALPHA dome flat (OC_MFLD_120820A_1_1_normal_normal_H_ALPHA.fits) without any rescaling of the image intensities.

With the exception of four dust rings and a difference in the global size of the vignetting from the central support

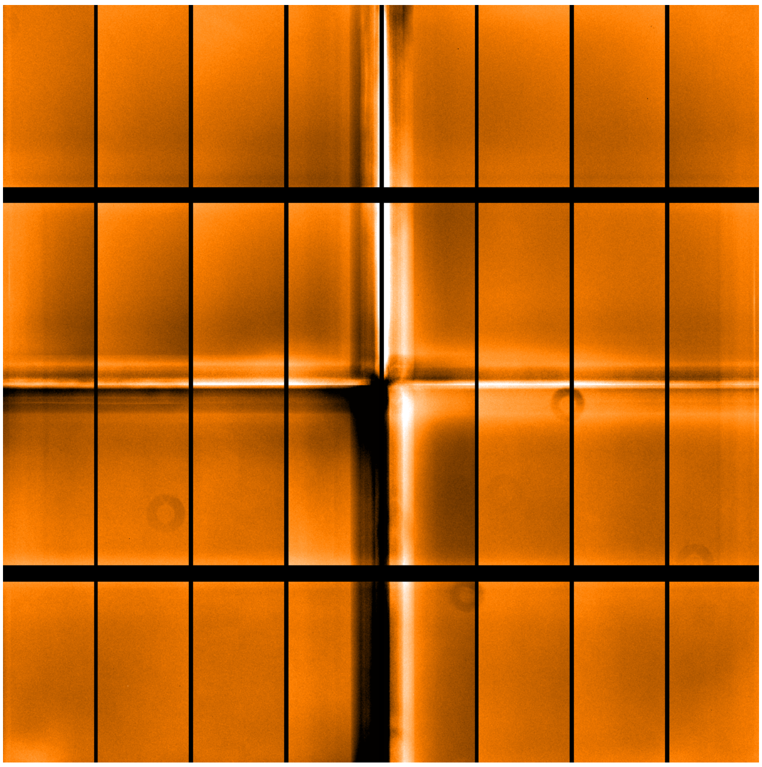

Figure 3: The ratio of a NB_659 and a H_ALPHA master dome flat. A recent NB_659 dome flat from 2012-08-22 (OC_MFLD_120822A_1_1_normal_normal_NB_659.fits) was divided by a H_ALPHA master dome flat from 2012-08-20 (OC_MFLD_120820A_1_1_normal_normal_H_ALPHA.fits). The image scaling of this figure is set tightly between 0.94 and 1.08 ($^{+8\%}_{-6\%}$). With the exception of some dust-induced rings and differences in the position and degree of vignetting, the NB_659 filter properties are very similar to those of the H_ALPHA filter. See figure 4 for a zoom of four representative detectors in this image.

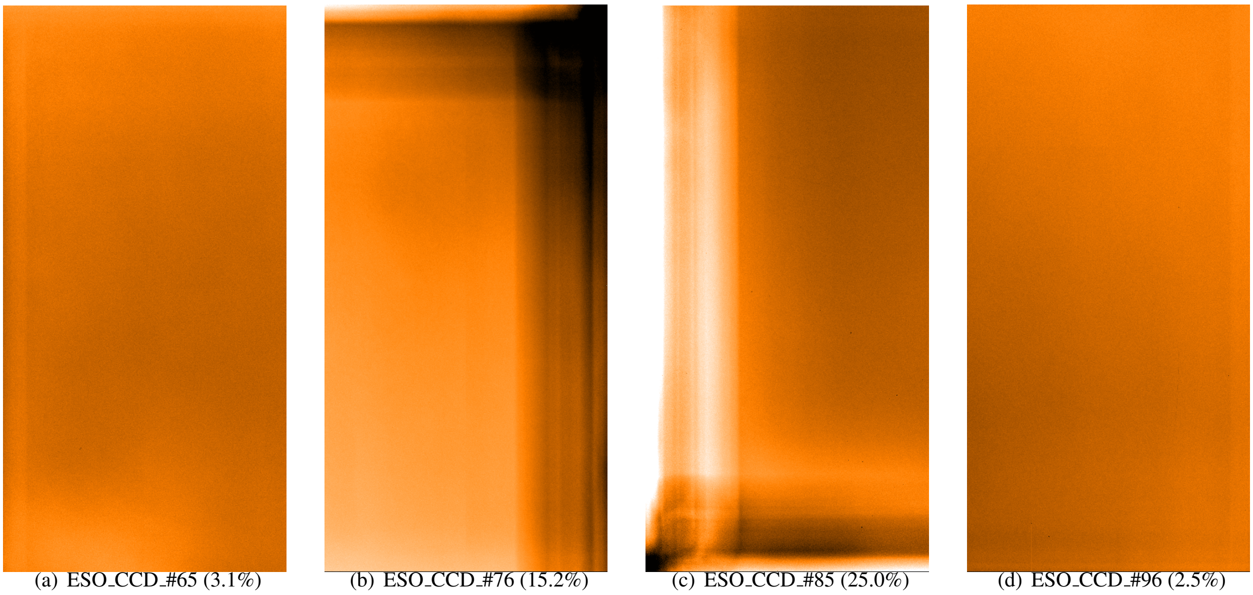

(a) ESO_CCD_#65 (3.1%) (b) ESO_CCD_#76 (15.2%) (c) ESO_CCD_#85 (25.0%) (d) ESO_CCD_#96 (2.5%)

Figure 4: A zoomed view of four detectors (ESO_CCD_#65, ESO_CCD_#76, ESO_CCD_#85, and ESO_CCD_#96) from the ratio of the two master NB_659 and H_ALPHA dome flats shown in figure 3. The image scaling has been set to lie between 0.94 and 1.08 $(^{+8\%}_{-6\%})$. The primary difference between the two filters lies in the position and degree of vignetting. The maximum flux variation across each detector is shown as a percentage in parentheses.

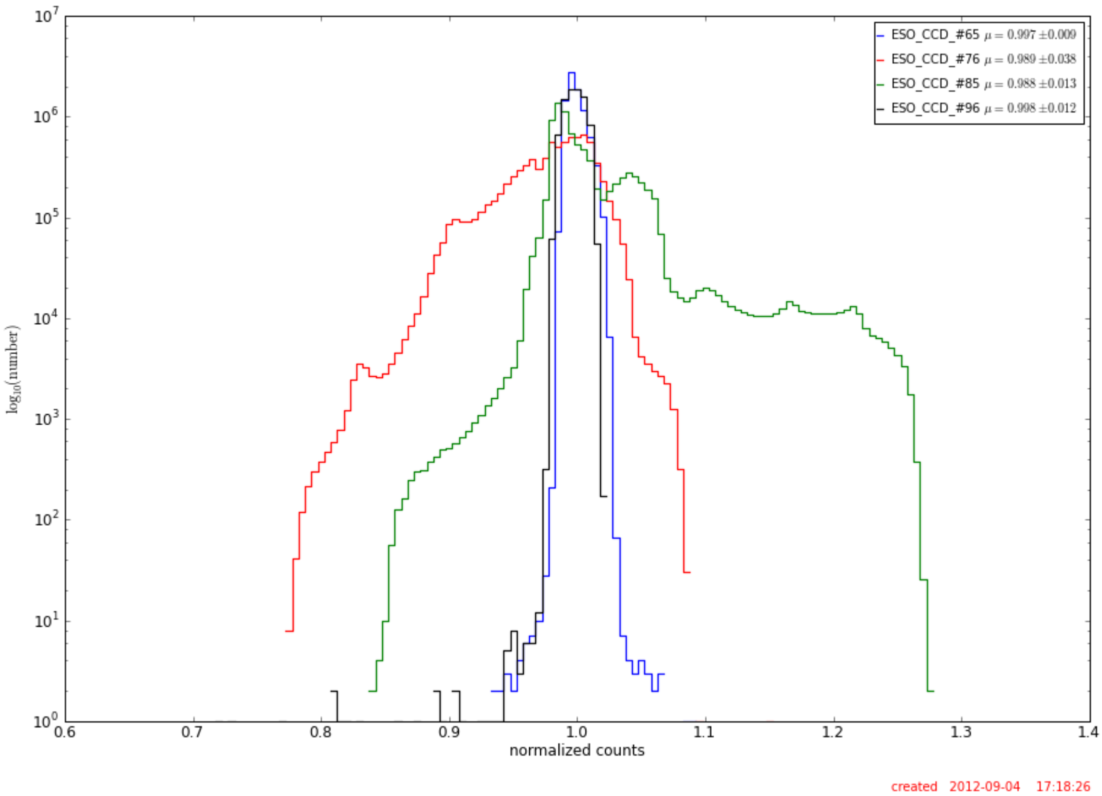

Figure 5: Histograms of the four detector ratios shown in figure 4.

structure, the two filters are very comparable. For detectors not affected by the vignetting cross, variations between the two filters are less than 3%. The worst-case central detectors, affected by the vignetting, differ by less than 25% (detector ESO_CCD_#85 shows the largest range in flux level differences). This latter effect, however, is most likely not due to variations in the filters themselves, but in the degrees of vignetting; either through slight differences in the shape of the central support or, most likely, in the angle by which the central supports are illuminated.

4 Long-Term Stability

Figure 6 shows a plot of the median flux, averaged over all 32 detectors, of NB_659 and H_ALPHA raw dome flats over a period of 10 months, from the start of operations to the end of August 2012. Raw dome flats are used instead of master dome flats, since the latter are normalized by the pipeline and all absolute flux level information is lost. All dome flat exposures for both filters were 7.0 seconds and did not change during this time period, so a direct comparison is rather easy. The NB_659 and H_ALPHA flux values are well-matched and, on average, differ by only 19.3 $\pm$ 12 ADU from one another.

There is a very noticeable decline of about 3000 ADU during the first 5 months of dome flat data. This decline is most likely due to a decrease in the dome flat lamp flux. This is either caused by a diminished output from the lamp itself, accumulated contamination (dust) on the reflective surfaces of the VST, or to a combination of both effects. Proof that this

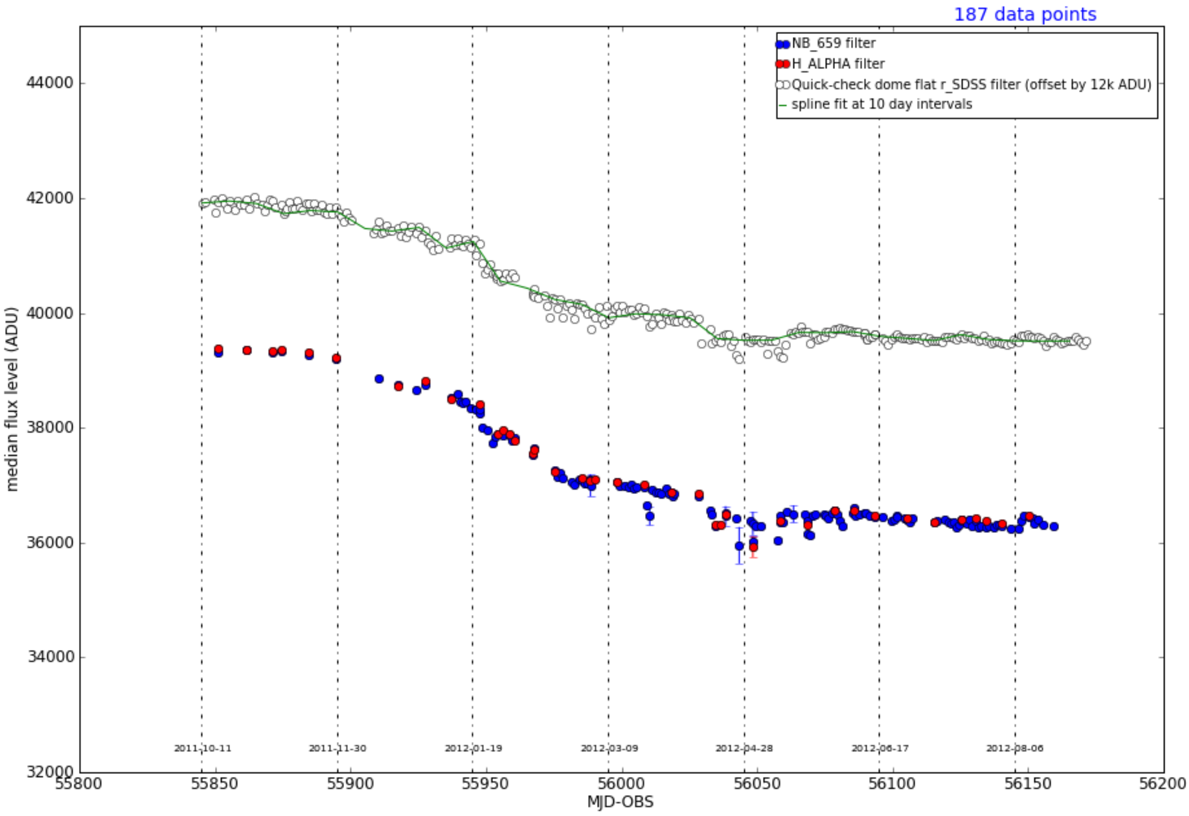

Figure 6: The median flux of the raw dome flats averaged over all 32 detectors for the NB_659 (blue points) and H_ALPHA filters (red points). This plot spans the range of dates from 2011-10-17 to 2012-08-20. All points are well matched for these two filters which only differ from one another by approximately 19 ADU (0.05%). All exposure times, for both filters, are 7.0 seconds and did not change during this period. The obvious decline is likely due to a decrease in the dome flat lamp flux as it is equally mapped for both filters. Proof that this decline is not due to changes in the NB_659 and H_ALPHA filters is given by the flux levels (arbitrarily scaled) of the quick-check dome flats obtained in the r′_SDSS band (open circles). A spline fit to the quick-check dome flat levels (r′_SDSS) was made at intervals of 10 days and is shown as a green line.

decline is not due to changes intrinsic to the NB_659 or H_ALPHA filters is given by the nearly identical flux level decline seen in the quick-check dome flats obtained in the r′_SDSS band (open circles in figure 6). The quick-check dome flats were chosen as a comparison to the NB_659 and H_ALPHA filters since the r′_SDSS band filter used in the quick-check dome flats includes the Hα wavelength region.

To remove the effect of this external decline in the dome flat lamp flux from any possible intrinsic variation within the NB_659 filter, a spline fit was made to the r′_SDSS band quick-check dome flat data. The interpolation between points every 10 days is shown as green line in figure 6). This fit was subtracted from the NB_659 dome flat data, which was then rescaled to the original median level of the NB_659 raw dome flats. In figure 7) this transforms the open circles to the solid circles. The median NB_659 raw dome flat level during this 10 month period then becomes 36462 $\pm$ 202 ADU and, therefore, the fluctuation of the NB_659 raw dome flux level about its median value is less than 0.6%.

There remains a slight residual decline in flux during this period, but this may simply be due to a colour difference between the NB_659 filter and the fit to the r′_SDSS filter. In any case, this residual decline is less than 560 ADU.

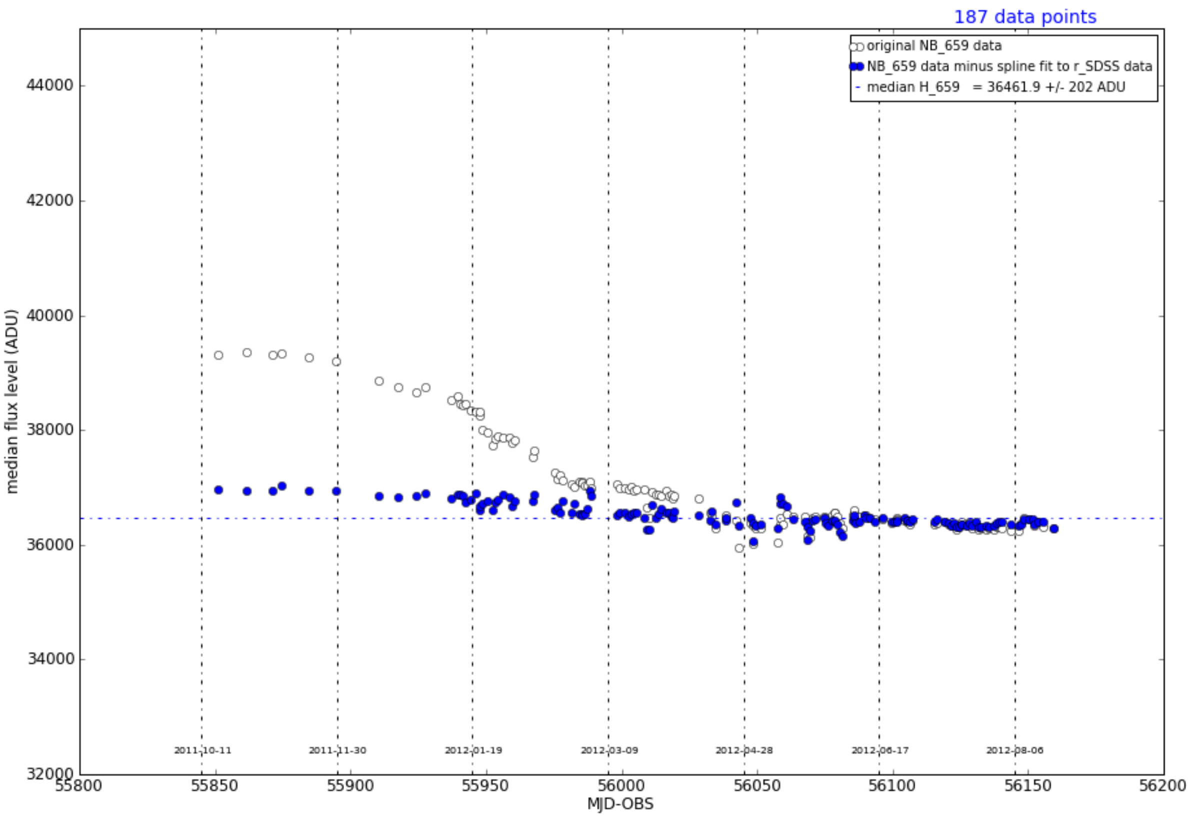

Figure 7: The same plot as figure 6 showing the original NB_659 raw dome flux as open points. The spline fit from the quick-check dome flat (green line in 6) is subtracted from each NB_659 raw dome flux point and then re-scaled to the median level of the NB_659 raw flats. The median level of the raw NB_659 dome flats is now 36462 $\pm$ 202 ADU.

Figure 8 shows a plot of the median zeropoints, averaged over all 32 detectors, of NB_659 and H_ALPHA standard star fields over a period of 5 months from the end of March 2012 to the end of August 2012. Data points from frames obtained in conditions other than PHOT or CLR were removed, as were points that were computed using 5 or less detected sources per CCD. For NB_659 this gives Z_{pt} = 23.1 $\pm$ 0.3. The zeropoints of the NB_659 and H_ALPHA filters differ from one another by only $\Delta\mathrm{mag} = 0.22 \pm 0.5$, although this comparison is difficult due to the small number of calibrated H_ALPHA standard star fields available (7 in total).

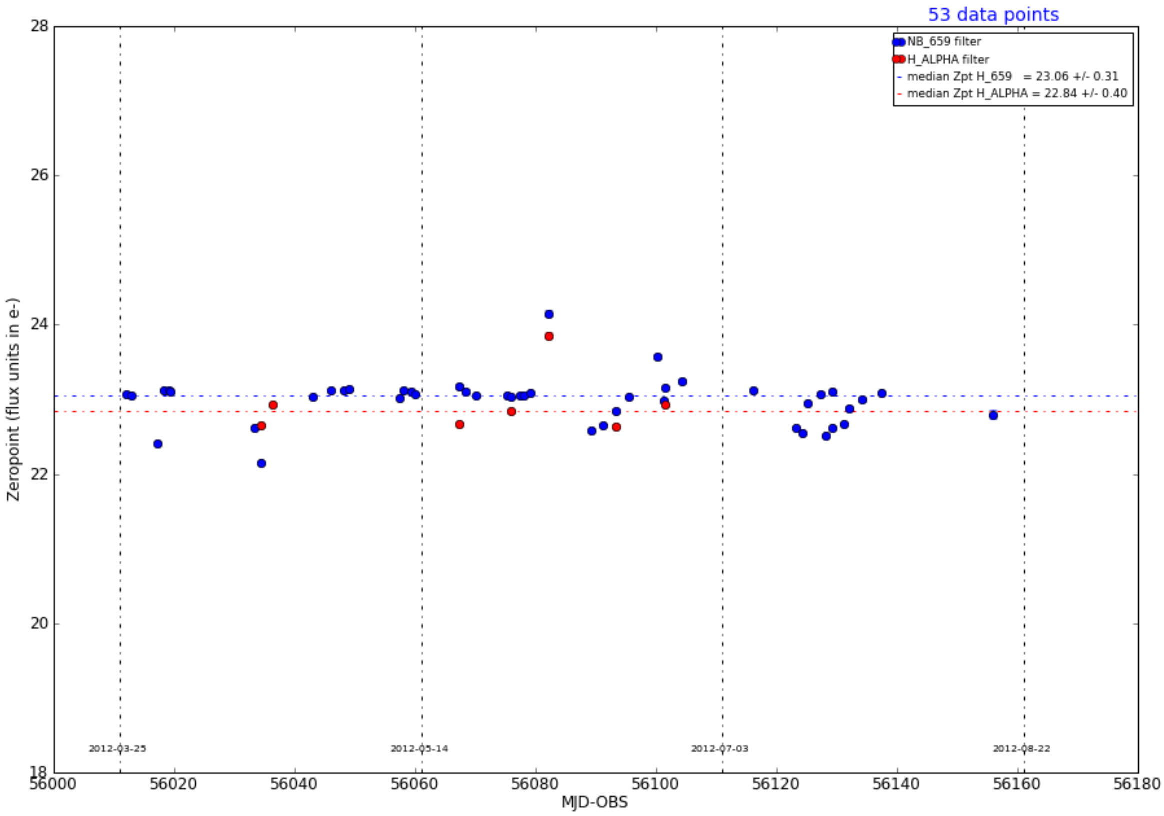

Figure 8: The median zeropoints (averaged over all 32 detectors) computed for standard fields in the NB_659 (blue points) and H_ALPHA filters (red points). This plot spans the range of dates from 2012-03-25 to 2012-08-20. The two filters have very similar zeropoint levels and differ only by $\Delta\mathrm{mag} \simeq 0.22 \pm 0.5$ (the large error is dominated by the fluctuations of the H_ALPHA values and is exacerbated by the small number of available H_ALPHA zeropoints).

Finally, a ratio was made of two master NB_659 dome flats separated from one another by 10 months. In figure 9 a master dome flat from Aug. 23, 2012 was divided by one obtained on Oct. 17, 2011. No rescaling of the resulting image was done. It is apparent from this figure that the NB_659 filter has remained very stable during this time interval. Only some changes in the dust-induced rings and a change in the vignetting are obvious. Variations in all detectors, unaffected by the vignetting in the support structure, are always less than 1%, while the affected central detectors never show differences between the maximum and minimum levels of more than 2.2%. The expanded views of four representative detectors in this ratio are shown in figure 10 and their intensity histograms are presented in figure 11.

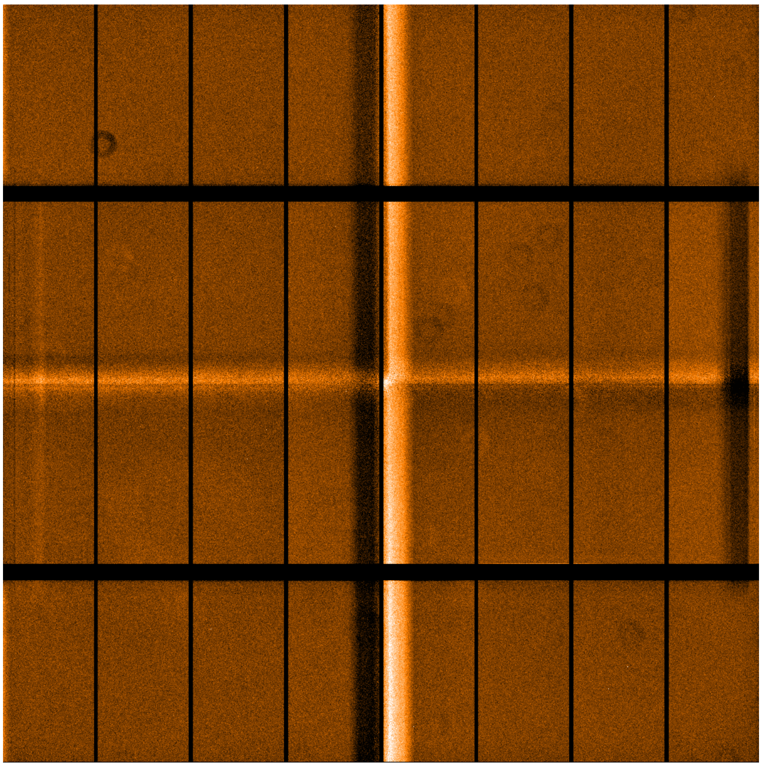

Figure 9: The ratio of two master NB_659 dome flats. A recent NB_659 dome flat from 2012-08-23 (OMEGA.2012-08-23T10:28:23.388.fits) was divided by a NB_659 master dome flat from 2011-10-17 (OMEGA.2011-10-17T07:47:50.586.fits). The image scaling is set very tightly between 0.99 and 1.03 ($^{+3\%}_{-1\%}$). With the exception of some dust-induced rings and slight changes in the vignetting, the NB_659 filter has remained very stable. See figure 10 for a zoom of four representative detectors in this image

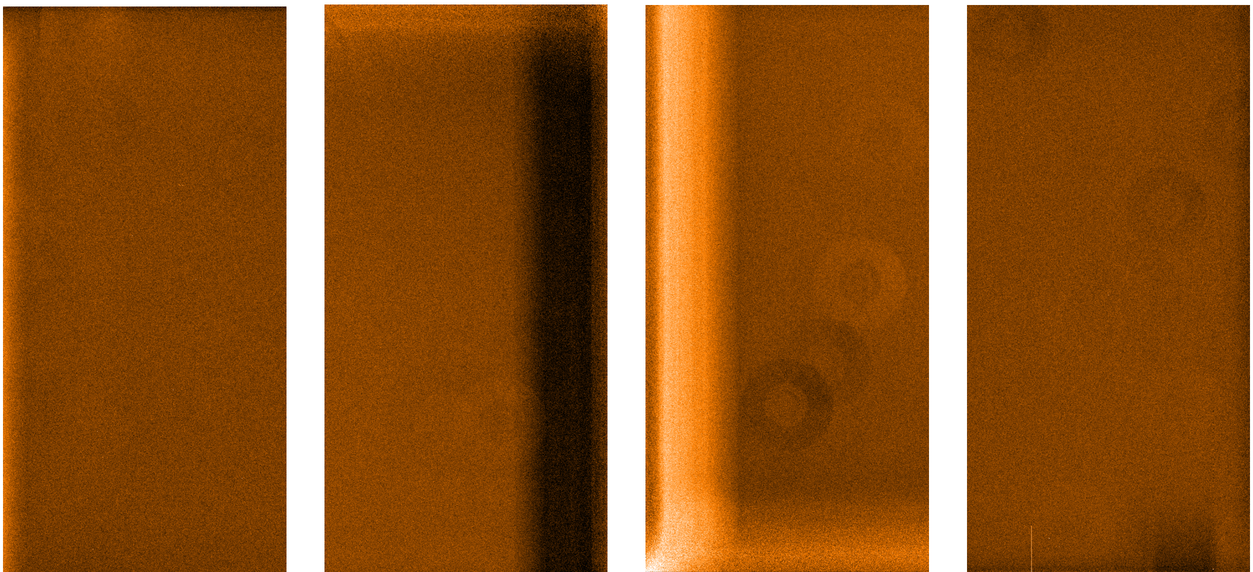

(a) ESO_CCD_#65 ($<1\%$) (b) ESO_CCD_#76 (1.5%) (c) ESO_CCD_#85 (2.0%) (d) ESO_CCD_#96 ($<1\%$)

Figure 10: A zoomed view of four detectors (ESO_CCD_#65, ESO_CCD_#76, ESO_CCD_#85, and ESO_CCD_#96) from the ratio of the two master NB_659 dome flats shown in figure 9. It is apparent that the NB_659 filter has remained very stable over the 10 months spanned by this ratio. The only changes appear to consist of dust rings and a change in the position of the vignetting produced by the central support structure. The full range of the intensity scale is between 0.99 and 1.03 ($^{+3\%}_{-1\%}$). The maximum flux variation (minimum to maximum level) across each detector is shown as a percentage in parentheses.

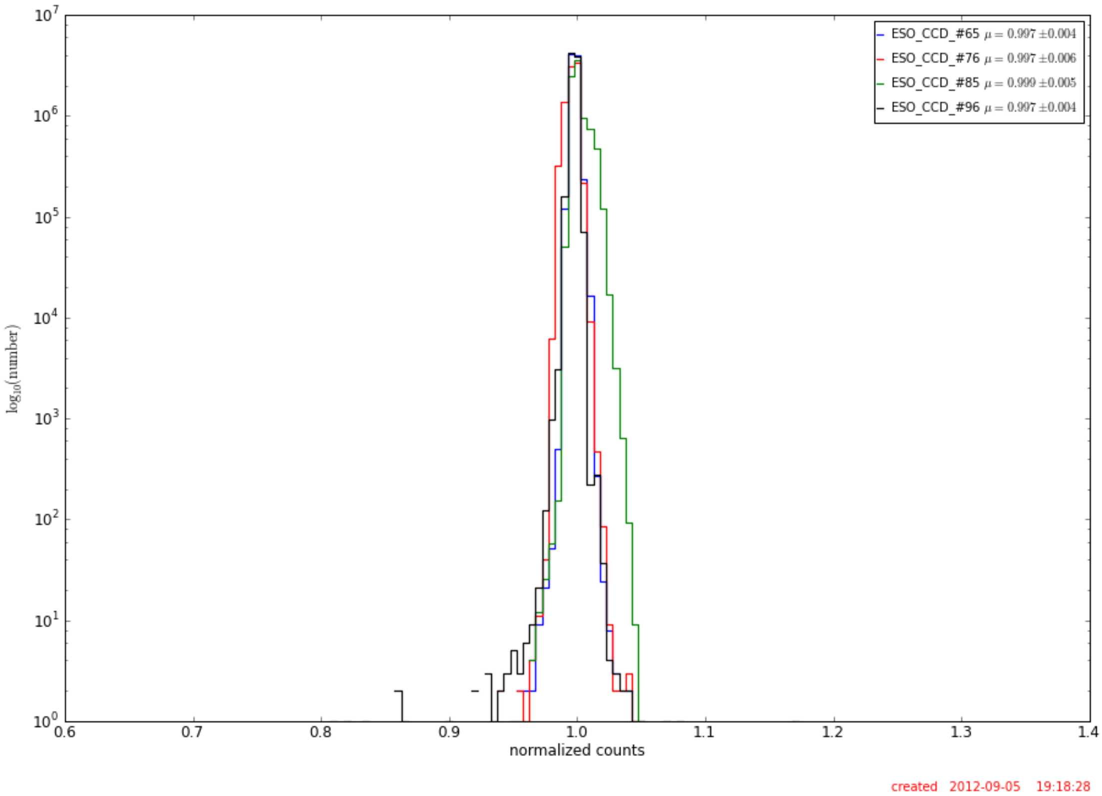

Figure 11: Histograms of the four detector ratios shown in figure 10.

References

Drew, J.E. & Greimel, R., OmegaCam Hα segmented filter tests. Review/analysis of lab appraisal carried out June-July 2009.

Martin, W. & Ilijevsky, I. OmegaCam Hα Mosaic Filter Test University of Munich. April 2011.

Mieske, S., et al., Very Large Telescope Paranal Science Operations OmegaCAM User Manual Doc. No. VST-MAN-OCM-23110-3110 Issue 90.1, Date 24/05/2012.